JOURNAL OF AGRICULTURAL AND FOOD CHEMISTRY

pubs.acs.org/JAFC Article

Fine Mapping and Candidate Gene Analysis of *Male Sterile 4* Promotes Complete Male Sterility in Common Wild Rice (*Oryza rufipogon*)

Amir Sohail,[†] Rongrong Qiao,[†] Xinyu Mao, Jinpeng Wan, Xiaochao Li, Chengkai lu,[*] and Peng Xu[*]

Cite This: *J. Agric. Food Chem.* 2025, 73, 28143−28152 Read Online

ACCESS | Metrics & More | Article Recommendations | Supporting Information

ABSTRACT: The transverse filament (TF) protein of the synaptonemal complex (SC) is crucial for rice meiosis, but its role in male sterility remains unexplored. We used Yuanjiang common wild rice (YJCWR) as a donor parent and developed a series of introgression lines (ILs, BC_4) in the genetic background of YUNDAO 1. *Male Sterile 4* (*MS4*) was mapped to a 49.8 kb region containing *OsZEP1* (*Os04g37960*), which encodes a transverse filament (TF) protein. Homozygous sterile lines exhibited shorter, weaker, pale yellow anthers and sterile pollens compared to fertile lines. SEM analysis reveals that *OsZEP1-CWR* impairs anther cuticle and pollen wall formation. Transverse semithin sections of sterile anthers show abnormal cuticle, pollen exine formation, delayed tapetum degradation, and defective microspores. CRISPR/Cas9 *OsZEP1* knockouts validated *OsZEP1* as the *MS4* candidate gene, causing complete male sterility. This study highlights the role of *MS4* in male fertility, and the newly developed KASP markers will be useful for marker-assisted breeding.

KEYWORDS: *rice, male sterility, fine mapping, MS4, SEM, CRISPR/Cas9*

INTRODUCTION

Male sterility is a phenomenon in which the stamens are malformed or degenerated and unable to produce functional pollen or male gametes.[1] Although male sterility is an unfavorable trait for the plant itself, it is indispensable for hybrid rice production, which produces 10% to 20% higher yield than conventional rice.[2] Sterile lines produce sterile pollen grains and are incapable of seed setting, making pollen development essential for the reproductive success of flowering plants. Pollen developed inside the male reproductive organ, anther, consists of four somatic layers of epidermis (E), endothecium (En), middle layer (ML), and tapetum (T), which encase microspore mother cells (MMCs) prior to meiosis.[3] During meiosis, four haploid microspores are generated from diploid pollen mother cells (PMCs) along with dynamic changes in the anther wall.[4] The mature pollen grain consists of the outer layer (exine) and the inner layer (intine). The exine consists of the outer layer (sexine), inner layer (nexine), and bacula that bridge the sexine and nexine. The pollen exine is composed of biopolymers of aliphatic lipids and phenolics, known as sporopollenin. Primexine, callose wall, and sporopollenin are three essential factors for pollen wall formation.[5] Although previous studies have focused on the microspore pollen wall, the potential functional mechanisms of development and function of microspores in male sterility remain unclear. Meiosis is a crucial event in sexually propagating eukaryotes by ensuring genome stability and genetic diversity in offspring.[6]

Rice serves as an excellent model for studying the molecular mechanisms underlying key events in meiosis, including meiosis initiation, sister chromatid cohesion, protection of centromeric cohesion, formation of meiotic DNA double-strand break (DSB), processing of meiotic DSB, DNA strand invasion or exchange, synaptonemal complex (SC), and crossover establishment. Although several genes have been reported for male sterility, only 28 meiosis-related genes have been characterized so far by map-based cloning, T-DNA insertion site tagging, RNAi, and CRISPR/Cas9, which caused male sterility in rice.[7] To date, only four genes named *HOMOLOGOUS PAIRING ABERRATION IN RICE MEIOSIS 2* (*PAIR2*), *HOMOLOGOUS PAIRING ABERRATION IN RICE MEIOSIS 3* (*PAIR3*), *CENTRAL REGION COMPONENT 1* (*CRC1*), and *zeaxanthin epoxidase 1* (*ZEP1*) have been reported to be involved in SC formation and cause male sterility.[8−11] *PAIR2* was the first cloned SC gene and is an ortholog of *Arabidopsis ASYNAPTIC 1* (*ASY1*) and the *S. cerevisiae HOMOLOGOUS PAIRING PROTEIN 1* (*HOP1*) gene that caused complete sterility due to synapsis failure in male and female meiosis.[12] Similarly, *PAIR3* also causes complete sterility in both male and female gametes due to abnormality in homology pairing and synapsis.[10] CRC1, an ortholog of *S. cerevisiae pachytene checkpoint 2* (*Pch2*) and *Mus musculus THYROID RECEPTOR-INTERACTING PROTEIN 13* (*TRIP13*), is a conserved SC component that leads to male sterility.[11] In rice, a homolog of *Arabidopsis ZYP1*, *ZEP1*, encodes a transverse filament (TF) protein of the SC.[13] TF

Received: August 2, 2025
Revised: October 17, 2025
Accepted: October 17, 2025
Published: October 23, 2025

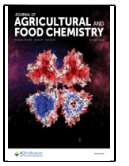

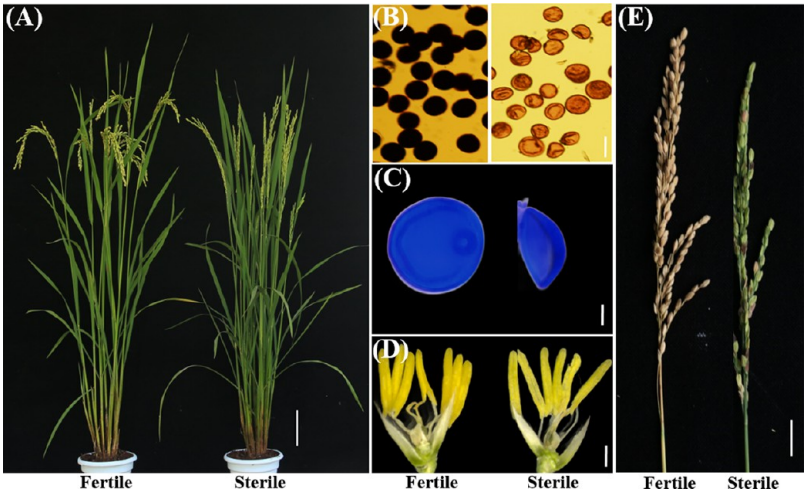

Figure 1. Phenotypic characterization of homozygous fertile and sterile lines in F_3 populations. Phenotypic comparison between fertile and sterile lines at heading stage (A). Pollen grains comparison of fertile and sterile lines stained with I_2−KI solution (B) and DAPI solution (C). Spikelets of fertile and sterile lines without lemma and palea (D). Panicle comparison of fertile and sterile at the maturity stage (E). Scale bars = 6 cm in (A and B); 100 μm in (C); 2 mm in (D), and 3 cm in (E).

proteins are essential for crossover formation, and TF-dependent crossovers exhibit genetic interference.[14] Previously, TF protein ZIP1 in budding yeast (*Saccharomyces cerevisiae*), Sycp1 in mice, c(3)G in *Drosophila* (*Drosophila melanogaster*), syp-1 in roundworm (*Caenorhabditis elegans*), ZYP1 in *Arabidopsis* (*Arabidopsis thaliana*), maize (*Zea mays*), barley (*Hordeum vulgare*), and wheat (*Triticum aestivum*), and ZEP1 in rice (*Oryza sativa*) have been reported.[13,15−23] The ZIP1 orthologs in plant species, including *Arabidopsis* and wheat, have not been associated with fertility, while barley showed semisterility and rice had complete sterility.

In this study, we identified *MS4* with a chromosomal segment from *Oryza rufipogon* variety YJCWR. We fine-mapped the *MS4* gene to a 49.4 kb region on chromosome 4, flanked by KASP markers KASP9 and KASP10, using an advanced $F_{2:3}$ (BC_4) population. The homozygous sterile line exhibited small, whitish anthers covered with densely packed cutin polymers. The microspores of sterile plants were shrunken with sporopollenin deposition, resulting in an irregular exine pattern, which indicates that disruption impairs anther cuticle and pollen wall formation, causing complete male sterility.

MATERIALS AND METHODS

Plant Materials and Growth Conditions. We developed numerous BC_4 introgression lines (ILs) using the *japonica* rice variety Yundao1 (YD1) as a recipient parent and Yuanjiang common wild rice (YJCWR, *O. rufipogon*) as a donor parent. Two of the ILs, U99, exhibited prostrate growth traits, while X-R displayed a stem-branch habit.[24] The IL (X-R) was crossed with the IL (U99) to develop F_1 and $F_{2:3}$ populations. We initially selected 99 plants (32 sterile and 67 fertile) from the F_2 population and genotyped them using the rice 20k chip assay (Figure S1). Genetic linkage analysis revealed a primary region on chromosome 4, spanning a 1805.5 kb interval between marker KASP1 and KASP16 (Figure 6B). A large $F_{2:3}$ population consisting of 2160 individuals was developed for fine mapping and progeny verification.

The YD1, IL (U99), IL(X-R), and $F_{2:3}$ populations were grown under natural field conditions at the breeding base of the Xishuangbanna Botanical Garden (XTBG), Menglun (21°56′ N, 101°15′ E), Yunnan, China, during 2024. The YD1 and two ILs were planted in a randomized complete block (RCB) design with three replications. Each replication consists of six rows of 1.98 m^2 and 12 plants row^{-1} with a density of 25 × 20 cm between each individual. Paddy field management, including irrigation, fertilization, disease, and pest control measures, was applied.

Iodine Potassium Iodide (I_2−KI) and 4′,6-Diamidino-2-phenylindole (DAPI) Staining of Rice Pollen. For I_2−KI and DAPI staining, rice panicles were fixed in Carnoy's solution (30% chloroform, 10% acetic acid, 57% ethanol, and 3% distilled water, V/V) for 2 h at room temperature and then stained in 1% I_2−KI and 5 $\mu g\ mL^{-1}$ DAPI solution. The I_2−KI-stained pollens were observed by using a microscopic imaging system (Olympus). The young panicles of F_2 homozygous fertile and homozygous sterile were stained in DAPI solution for meiotic chromosome observation and processed according to Wu et al.[25] Pollen fertility was calculated as the total number of stained pollen grains divided by the total number of pollen grains examined. Spikelet fertility was calculated as the total number of filled spikelets per panicle divided by the total number of spikelets per panicle.

Scanning Electron Microscopy (SEM). For the SEM assay, anthers of F_2 homozygous fertile and homozygous sterile lines were fixed overnight in 2.5% (v/v) glutaraldehyde solution in 0.1 M sodium phosphate buffer at 4 °C, then dehydrated through a graded ethanol series (30−100%), and exchanged three times with isoamyl acetate, following the protocol described by Khan et al.[26] After dehydration, the samples were critical point dried, coated with gold palladium in a Hitachi E-1010 ion sputter for 5−10 min, and then observed and photographed using SEM (Hitachi TM-1000) at the central laboratory of the Xishuangbanna Tropical Botanical Garden, Menglun, Yunnan, China.

Semithin Sectioning. The rice spikelets from $F_{2:3}$ homozygous fertile and homozygous sterile lines at different developmental stages were fixed in FAA (Formalin acetic alcohol solution, formalin: acetic acid: 70% ethanol 1:1:18, V/V) solution for 2 days at room temperature and then dehydrated in 50, 60, 70, 85, and 90% (V/V) ethanol for 30 min each, followed by 100% (V/V) ethanol for 1 h as previously described by Khan et al.[26] The samples were embedded with Technovit glycol methacrylate 7100 resin and polymerized at 60 °C for 3 days. Sections of 2 μm thickness were cut using an RM2265 rotary microtome (Leica, Germany), stained in 0.25% toluidine blue dye for 30 s, and observed under a Leica DM2000 microscope.

DNA Extraction and KASP Marker Development. Genomic DNA was extracted from young leaves using the cetyltrimethylammonium bromide (CTAB) method.[27] DNA concentrations were measured using a Nanodrop one spectrophotometer (Thermo Fisher Scientific, USA) and adjusted to a final working concentration of 5

https://doi.org/10.1021/acs.jafc.5c09809
J. Agric. Food Chem. 2025, 73, 28143−28152

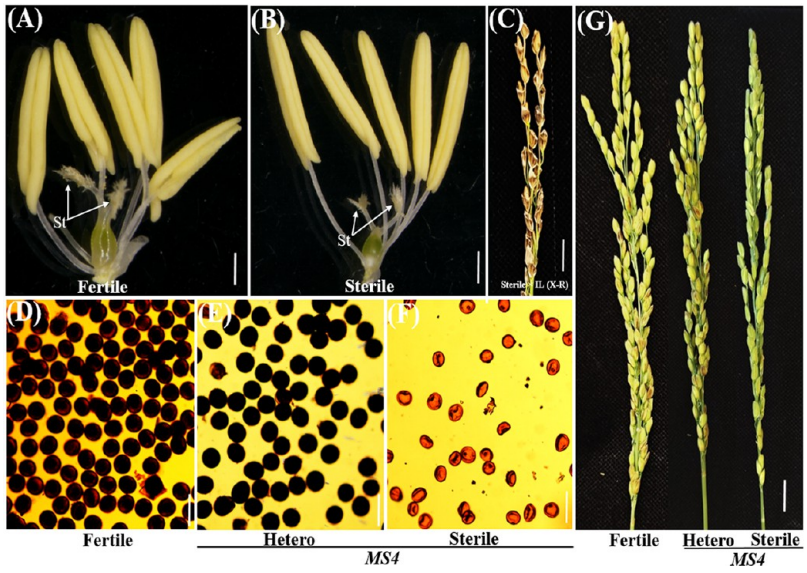

Figure 2. Reproductive organ comparison of homozygous fertile and sterile lines of F_3. Spikelets of fertile and sterile without lemma and palea (A, B). Panicle of sterile × ILs (X-R) (BC_1F_1) at maturity (C). Pollen comparison of homozygous fertile line (D), heterozygous (E), and sterile line (F) stained with I_2−KI solution. Panicle of homozygous fertile, heterozygous, and homozygous sterile lines at milky stage (G). Bars = 2 mm in (A, B); 2 cm (C); 100 μm in (D−F); 3 cm in (G). st = stigma.

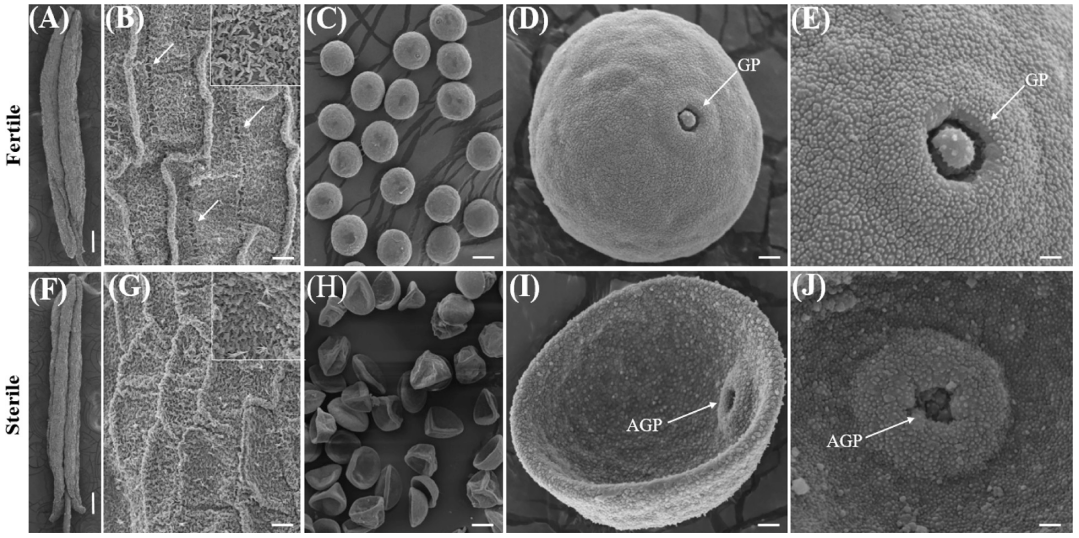

Figure 3. SEM analysis of anthers and pollen grains in homozygous fertile and sterile lines at stage 13. (A, F) Anthers from the fertile (A) and sterile (F) lines. Scale bars: 200 μm. (B, G) Epidermal surface of the fertile (B) and sterile (G) lines. Scale bars: 10 μm. (C, H) Pollen grains of the fertile (C) and sterile (H) lines. Scale bars: 30 μm. (D, I) Enlarged view of a single pollen grain of fertile (D) and sterile (I) lines. Scale bars: 4 μm. (E, J) Enlarged surface of pollen exine and germination pore (GP) of the fertile (E) and sterile (J) lines. Bars 2 μm.

ng/L. For fine mapping of *MS4*, 16 kompetitive allele-specific PCR (KASP) markers (Table S2) in the region of 1805.45 kb between KASP1-KASP16 markers on chromosome q4 of *Oryza sativa Japonica* were developed from polymorphic SNPs between the ILs (U99) and ILs (X-R) parents using Primer 3 (https://junli.netlify.app/apps/design-primers-with-primer3/). KASP primers were designed using approximately 200 bp sequences flanking the SNP locus, in accordance with the standard KASP guidelines provided by LGC Limited, UK. Standard FAM and HEX probes were conjugated with the allele-specific primers at the target SNP (Table S2). The primers used for genomic and promoter amplification of *ZEP1* are shown in Table S3.

KASP PCR. Polymerase chain reaction (PCR) was performed in a 5 μL reaction volume consisting of 2.43 μL of 2 × Master mix VI, 0.07 μL of primers (0.023 μL forward 1, 0.023 forward 2, and 0.023 reverse primer), and 2.5 μL of DNA. PCR application was performed using a Hydrocycler[2] (LGC Limited, UK) with activation at 93 °C for 15 min with one cycle, followed by 10 cycles (denaturation at 93 °C, 20 s, annealing at 61−55 °C, 60 s (drop 0.06 °C per cycle), followed by 26 cycles (denaturation at 94 °C, 20 s, annealing at 55 °C, 60 s). Fluorescence intensity and luminescence of the PCR plate were read using a FLUOstar Omega SNP reader and visualized with KlusterCaller genotyping software (LGC Limited, UK).

Generation of *zep1* Mutant Using the CRISPR/Cas9 System. The CRISPR/Cas9 system was used to knock out *ZEP1* according to the methods previously described by Miao et al.[28] The 23-bp sgRNA: Cas9 two target sequences of *ZEP1* were introduced into the pYLsgRNA-OsU6a and pYLsgRNA-OsU3m vectors. The final vector was transformed into YD1 using Agrobacterium-mediated transformation.[29] The primers used are listed in Table S4.

Statistical Analysis. The experimental data were analyzed using SPSS v.20 software (IBM) and GraphPad Prism 7. The Chi-square

https://doi.org/10.1021/acs.jafc.5c09809
J. Agric. Food Chem. 2025, 73, 28143−28152

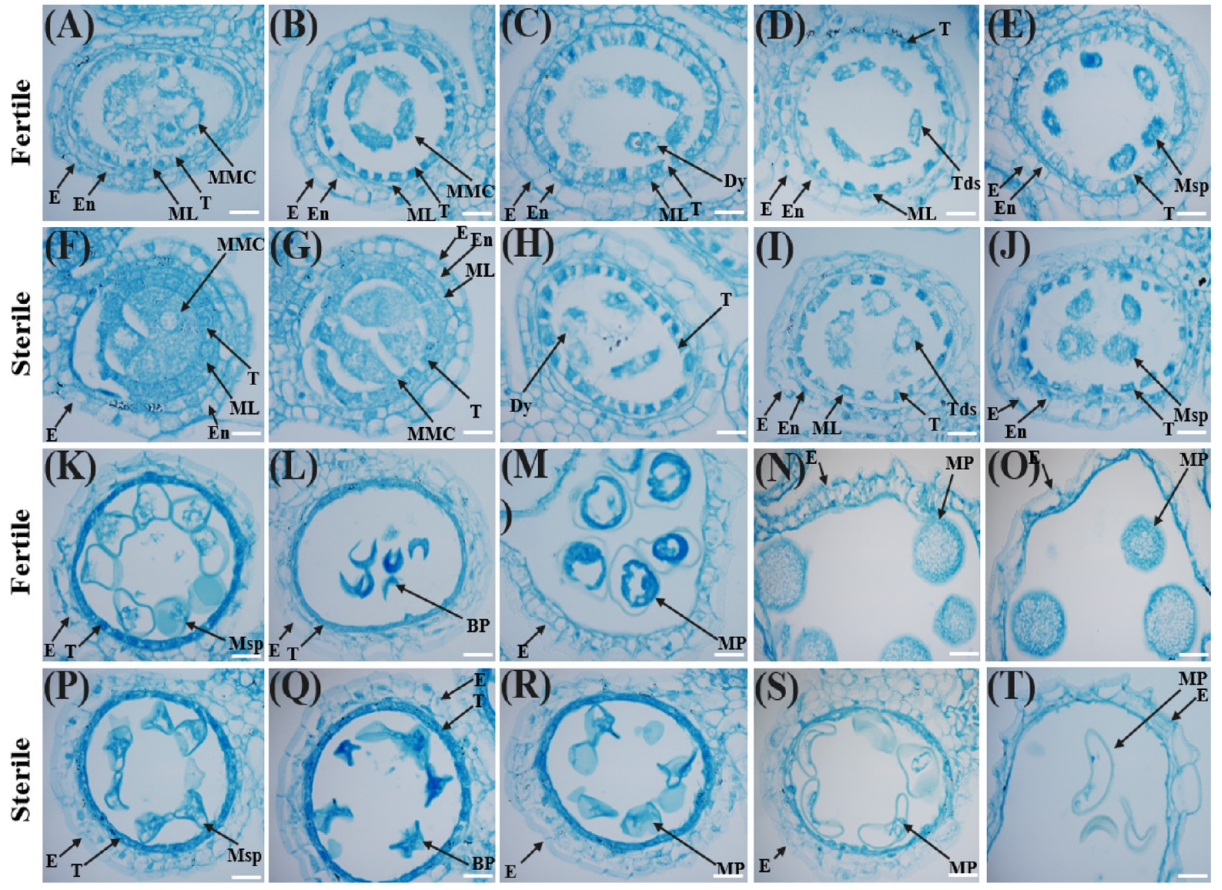

Figure 4. Semithin sections analysis of anther development in homozygous fertile and sterile lines. Anther sections of fertile (A–E, K–O) and sterile (F–J, P–T) lines at stages 6, 7, 8a, 8b, and 9–14, respectively. E = epidermis; En = endothecium; Msp = microspore; ML = middle layer; T = tapetum; Dy = dyad; Tds = tetrad; Msp = microspore parietal cell; BP = bicellular pollen; MP = mature pollen. Scale bars = 10 μm.

(χ^2) test was used to determine the segregation ratio of the population. Student's *t* test was employed to analyze statistically significant differences at 5% and 1% probability levels, respectively. Sequence alignment was performed by using SnapGene software.

RESULTS

Identification and Characterization of *MS4*. The sterile plant of F_2 showed normal vegetative growth like a fertile plant based on the plant morphology (Figure 1A). However, during the reproductive stage, the spikelets of the sterile plant exhibited complete sterility (Figure 1E). The pollen grains of the sterile plant were shrunken and empty and could not be stained with 1% iodine potassium iodide solution (I_2–KI) (Figure 1B). Additionally, the sterile pollens appeared abnormal when stained with 4′,6-diamidino-2-phenylindole (DAPI) (Figure 1C). The anther of the sterile plant was weaker, shorter, pale yellow, and failed to produce viable pollen grains when compared to the fertile plant (Figure 1D). The sterile plant displayed a reduced seed setting (~5%), primarily caused by inviable pollen grains (~99%) at maturity (Figure 1E, Figure S2). When the sterile plant was pollinated with IL (X-R), all the F_1 progenies were fertile (Figure 2A–C), indicating that the *MS4* sterile plants possessed normal female fertility and the phenotype is controlled by a single recessive gene (Figure 2D–G, Table S1).

Scanning Electron Microscopy (SEM) of *MS4* Anthers and Pollen Grains. To further confirm the morphological difference in the anther and pollen grains of F_2 homozygous fertile and homozygous sterile plants, SEM was performed on mature anthers and pollen grains at stage 13 (Figure 3). In contrast to the well-developed anther epidermis of fertile plants, which exhibited a less compact, spaghetti-like pattern of cutin layers with longer cells (Figure 3A,F), the epidermis of sterile anther was covered with a dense arrangement of cutin layers, making the epidermis more compact (Figure 3B,G). The fertile pollen grains were round and enlarged with starch, and their exine developed uniformly with sporopollenin granules embedded in the extracellular matrix (Figure 3C,D). In contrast, the sterile pollen grains were shriveled, with disorganized sporopollenin deposition, resulting in an irregular exine pattern (Figure 3H,I). The fertile microspores had normal germination pores, while the sterile microspores exhibited abnormal germination pores (Figure 3E,J). These SEM results indicate that disruption in *OsZEP1* impairs both the anther cuticle and pollen wall formation.

Transverse Semithin Section Analysis of the *MS4*. To characterize the morphological defects in the sterile plant, we examined transverse semithin sections of fertile and sterile anthers at different developmental stages of pollen. No significant differences were observed between the fertile and sterile anthers until the early microspore stage (Figure 4A,F). At this stage, the tapetal cells of the fertile anther become condensed and deeply stained, while the middle layer (ML) was barely visible compared to the sterile anther (Figure 4B,G). The pollen mother cells (PMCs) of fertile plants underwent normal meiosis and formed tetrads, whereas the

https://doi.org/10.1021/acs.jafc.5c09809
J. Agric. Food Chem. 2025, 73, 28143–28152

sterile plants exhibited abnormal meiosis and formed triads (Figure 4C,D,H,I). At stage 9, the young microspores were successfully released from tetrads in the sterile anthers, but they remained shrunken and deshaped. The tapetal cells of sterile were condensed and less vacuolated, and the middle layer had completely disappeared, similar to fertile anther (Figure 4E,J). At stage 10, the fertile tapetum became thinner, and the microspores exhibited vacuolation, enlarging, and becoming round in shape (Figure 4K).

In contrast, the tapetum in sterile anthers displayed slight expansion and dark staining, and the microspores retained an irregular shape (Figure 4P). At stage 11, the microspores in the fertile anthers underwent the first mitotic division, forming normal bicellular pollen, while the sterile ones formed abnormal bicellular pollen (Figure 4L,Q). At the mature pollen stage, the fertile mature pollen grains were filled with starch granules and densely stained, and the tapetum had disappeared. However, in sterile anthers, the endothecium cells expanded, the tapetum abnormally persisted, and MPs degenerated into irregular, shrunken shapes without starch granules (Figure 4M−O,R−T). In fertile anthers, the two adjacent pollen sacs merged into a single locule. In contrast, the pollen sacs of sterile plants remained separated, and aborted pollen grains were released through individual stomia, indicating that antiher dehiscence was also affected in sterile plants (Figure S3A,B). These results indicate that defects in Msp formation and anther development caused sterility.

Meiotic Products Analysis of the *MS4*. To explore the potential role of the male sterility gene in bipolar spindle assembly during meiotic product formation, we examined the chromosome separation and spindle organization in both fertile and sterile lines of the male sterility gene using acetocarmine staining. In the fertile line, homologous chromosomes segregated and formed a dyad in telophase I (Figure 5A), and tetrad formation occurred at the end of meiosis II (Figure 5B). In contrast, the sterile line exhibited a dyad and triad at the telophases I and II (Figure 5C,D). The meiocytes of sterile plants showed an unbalanced tetrad configuration at telophase II, with triads also present in the sterile line.

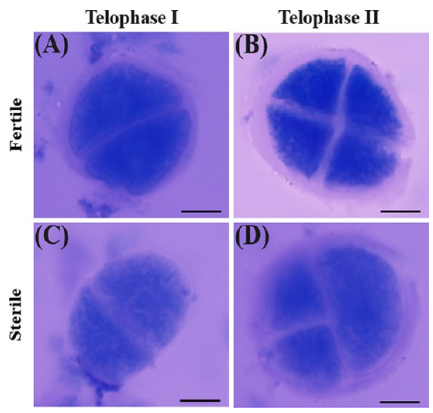

Figure 5. Meiotic product analysis of homozygous fertile and sterile lines. Dyads and tetrads form at telophase I and telophase II of the fertile line, respectively (A, B). Dyads and triads form at telophase I and telophase II of the sterile line, respectively (C, D). Scale bars: 10 μm.

Map-Based Cloning of *MS4*. To identify a new male sterility gene, we constructed two ILs named IL (X-R) and IL (U99), which carry segments from *O. rufipogon* Griff. in the genetic background of YD1 (Figure S1). Both ILs were crossed, and the heterozygous F_1 plants were self-pollinated to generate the F_2 population for fine mapping. Furthermore, the $F_{2:3}$ population showed a fertile-to-sterile segregation ratio of 3:1 (1619 fertile and 541 sterile plants), which conformed to the Mendelian ratio (Table S1), indicating that a single recessive gene controls the phenotype.

To fine-map the candidate gene, we initially selected 32 sterile plants and 67 fertile plants from the F_2 population and genotyped using the rice 20k chip assay (Figure S1). QTL scans were performed using the selected model and at the specified step size, with a threshold LOD score of 3.[30] Preliminary linkage analysis revealed that the putative candidate region was located on the long arm of chromosome 4 (Figure 6A), spanning an 1805.5 kb interval between KASP markers KASP1 (213,37,500 bp) and KASP16 (231,42,975 bp) (Figure S1, Figure 6A).

To narrow down the interval, 2160 individuals from the $F_{2:3}$ population were genotyped using 16 polymorphic KASP markers (KASP1-KASP16), and the interval was mapped to a 49.8 kb region flanked by markers KASP9 (225,81,608 bp) and KASP10 (226,31,426 bp) (Figure 6B; Figure S4A,B). The 133 recombinants were classified into 33 groups based on the genotypes (Figure 6C). Recombinants L6 and L26 were sterile, which helped delimit the *MS4* gene to the upstream side of the KASP11 marker. Similarly, L10 and L24 narrowed the *MS4* gene to the downstream side of KASP8. Additionally, recombinant L8 and L25, which contained the YJCWR allele at the KASP9 and KASP10 markers, exhibited sterility. The fine mapping results from all recombinant groups ultimately confined *MS4* to a 49.8 kb genomic region flanked by KASP9 and KASP10 (Figure 6C). These recombinants were then used for progeny testing to confirm the fine mapping results.

Candidate Gene Analysis of *MS4* and Validation Using CRISPR/Cas9. A candidate gene search using the physical position of the two flanking markers identified during the fine mapping (KASP9 and KASP10) in the Gramene database (https: //www.gramene.org/ (accessed on 20 May 2025)) using the *Oryza sativa* japonica group reference genome identified seven predicted genes that fell within the 49.8 kb region (4:225,81,608−226,31,426) of *MS4* (Figure 6D and Table 1). Additionally, according to the Rice Genomic Annotation Project Database (RGAP, https://rice.plantbiology.msu.edu/a) and Rice Annotation Project Database (RAP-DB, https://rapdb.dna.afrc.go.jp/), there were seven possible candidate genes (*LOC_Os04g37960*, *LOC_Os04g37970*, *LOC_Os04g37980*, *LOC_Os04g37990*, *LOC_Os04g38000*, *LOC_Os04g38010*, and *LOC_Os04g38026*) in the 49.8 kb genomic region (Figure 6D). Among these, five genes were predicated to encode monosaccharide transporter (STP subfamily), speciated STP protein 1, 14, 15, 16, and 17. One gene is putatively associated with an expressed protein, while *LOC_Os04g37960* is predicated to encode a transverse filament (TF) protein (Table 1).

Since *Os04g37960* (*ZEP1*) was potentially related to male sterility, we amplified the genomic DNA sequence of this gene, including its promoter region (Table S3). Sequence comparison of seven candidate genes between the two parents, IL (X-R) and IL (U99), revealed a base substitution (C/A) in the promoter of *ZEP1* and a synonymous SNP (C/A) in the coding sequence of STP17, based on the Nipponbare reference genome sequence (www.gramene.org) (Figure 6E, Table 1,

https://doi.org/10.1021/acs.jafc.5c09809
J. Agric. Food Chem. 2025, 73, 28143−28152

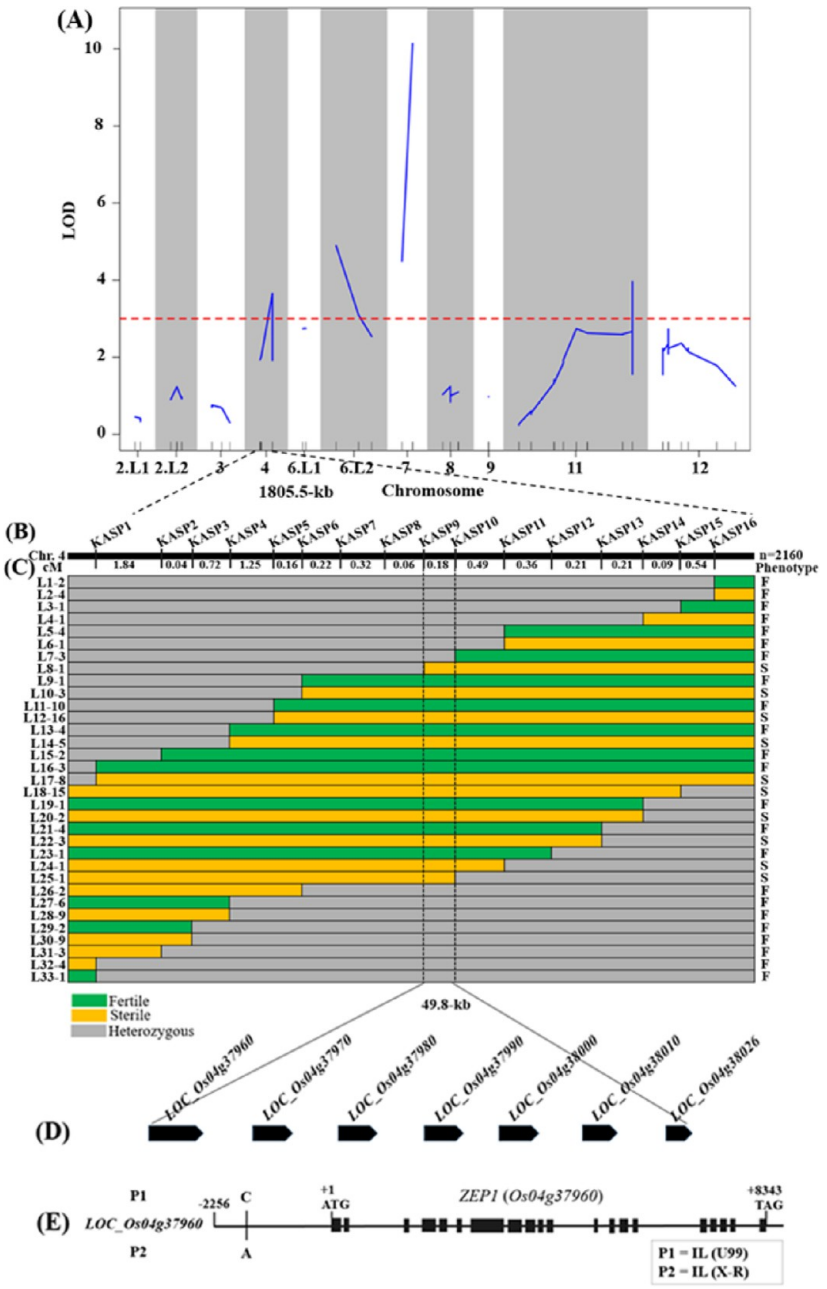

Figure 6. Fine mapping of *MS4* on chromosome 4 in rice. A major QTL of male sterility was identified on chromosome 4 using 99 individuals of the F_2 population based on bulked segregant analysis (A). High-resolution linkage map of the *MS4* region using 2054 individuals of F_3 populations (B). Genotype and phenotype of recombinants for fine mapping; the allele was fine-mapped to a 49.8 kb region between markers KASP9 and KASP10. The green, yellow, and gray bars represent the marker genotypes of fertile, sterile, and heterozygous, respectively. F and S indicate fertile and sterile phenotypes, respectively (C). Seven possible putative genes in the target region of *MS4* (D). Structure and mutated site of candidate gene *LOC_Os04g37960* between P1 and P2; the black boxes and lines represent exons and introns, respectively (E).

Table 1. Candidate Genes Located within 49.8 kb Physical Regions of *MS4* on Chromosome 4

locus ID	position	annotation	promoter diff.	coding region diff.
Os04g37960	22583456−22592933	transverse filament (TF) protein	1 SNP	no difference
Os04g37970	22594108−22595839	monosaccharide transporter (STP subfamily); STP protein 14	not sequenced	no difference
Os04g37980	22598600−22601305	monosaccharide transporter 1 (STP subfamily); STP protein 1	not sequenced	no difference
Os04g37990	22611843−22620016	SUGAR TRANSPORT PROTEIN 15; STP protein 15	not sequenced	no difference
Os04g38000	22622402−22622766	expressed protein	not sequenced	no difference
Os04g38010	22626439−22628157	monosaccharide transporter (STP subfamily); STP protein 16	not sequenced	no difference
Os04g38026	22633284−22627207	monosaccharide transporter (STP subfamily); STP protein 17	not sequenced	1 synonymous SNP

https://doi.org/10.1021/acs.jafc.5c09809
J. Agric. Food Chem. 2025, 73, 28143−28152

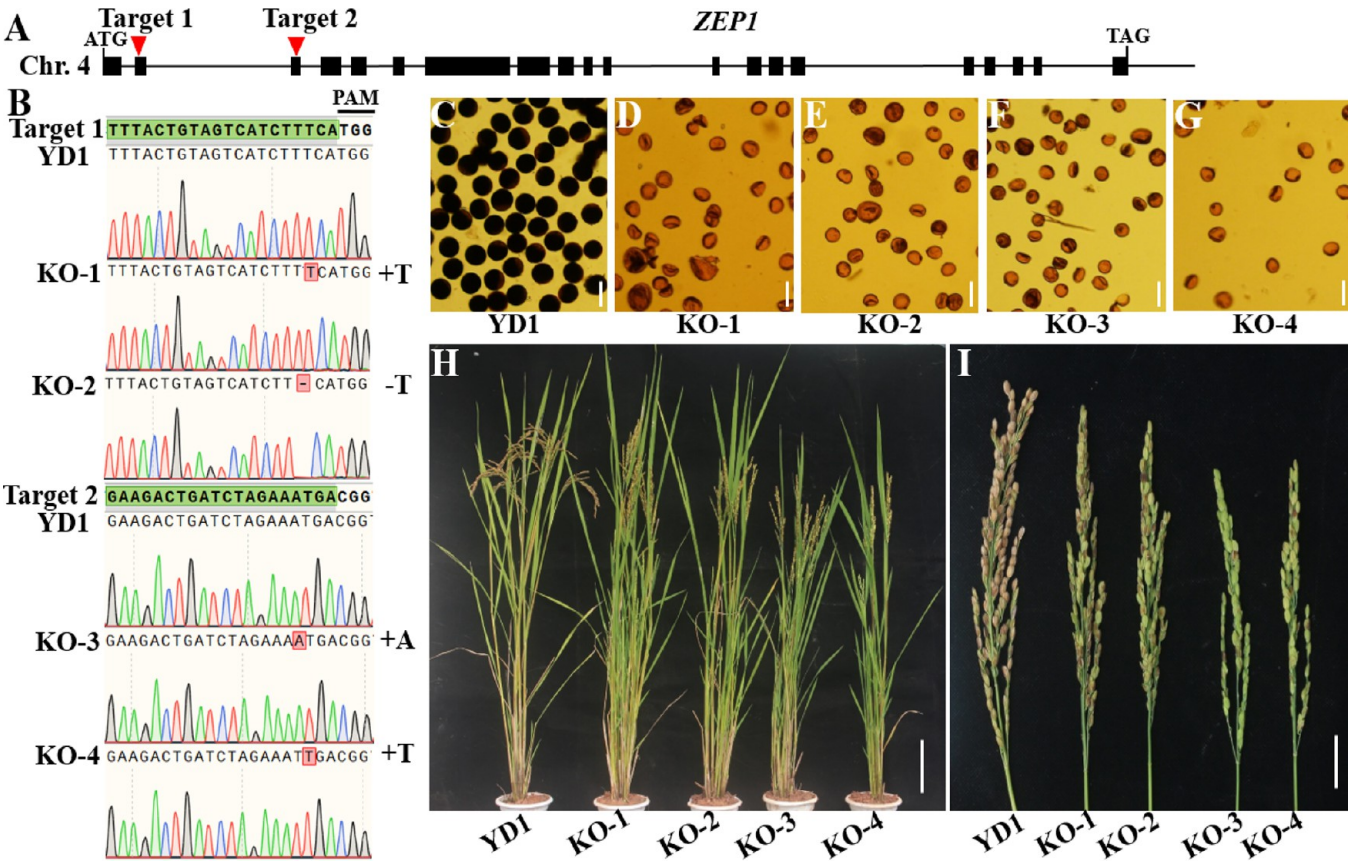

Figure 7. CRISPR/Cas9-mediated knockouts of the *ZEP1* gene and its phenotypic characterization. Schematic of the *ZEP1* gene with the sgRNA: Cas9 targets (red arrow and green sequences) and corresponding protospacer-adjacent motif (PAM) sequences (underlined) designed in the second and third exon using the CRISPR/Cas9 system. Four homozygous knockouts (KO1, KO2, KO3, and KO4) of *ZEP1* were obtained in YD1 background using CRISPR/Cas9 system. The nucleotide changes were highlighted in red with "−" and "+" indicating deletion and insertion, respectively (A, B). Pollen grains comparison of YD1 and knockout lines KO1, KO2, KO3, and KO4 stained with I_2−KI solution (C−G). Phenotype comparison of YD1 and four knockout lines of *ZEP1* at the maturity stage (H), and panicle length (I). Scale bars 100 μm in (C−G), 30 cm in (H), and 3 cm in (I).

Table S3). No sequence differences were found between the two parents in the other five loci (*LOC_Os04g37970*, *LOC_Os04g37980*, *LOC_Os04g37990*, *LOC_Os04g38000*, and *LOC_Os04g38010*) (Table 1).

Furthermore, *LOC_Os04g37960* was further confirmed as the *ZEP1* gene by targeted knockout using a CRISPR/Cas9 system. The gRNA/Cas9 vector targeting the specific site of *LOC_Os04g37960* on the second and third exons were introduced into YD1. Sequencing analysis revealed four homozygous knockout lines: KO1 (+T), KO2 (-T), KO3 (+A), and KO4 (+T) (Figure 7A,B). The four knockout lines showed complete male sterility with empty pollen grains and no seed sitting compared to the YD1 phenotype (Figure 7C−I). Taken together, these results confirmed that *LOC_Os04g37960/ZEP1* is the target gene whose mutation can cause the complete male sterile phenotype.

DISCUSSION

Male sterility is a valuable trait for hybrid seed production. The identification and characterization of male-sterile genes underlying molecular mechanisms affecting male sterility are critical for heterosis and ensure food security.[2] Meiosis is essential for sexual reproduction, involving processes such as homologous pairing, synapsis, recombination, and segregation.[31] Defects in male meiosis can reduce fertility.[32] Here, we discovered *MS4*, which regulates male sterility and was fine-mapped to a physical distance of 49.8 kb on the long arm of chromosome 4. The YJCWR allele at the *MS4* locus negatively regulates male fertility in rice. Among the candidate genes, *ZEP1* encodes the transverse filament (TF) protein of the synaptonemal complex protein 2, which may play an important role in male sterility in rice.[13] The sterile line exhibits shorter, weaker, and pale yellow anthers and produces completely sterile pollen due to defects in the anther cuticle, pollen exine formation, and delayed tapetum degradation.

ZEP1, an ortholog of *S. cerevisiae* ZIP1 and *Arabidopsis* ZYP1, is essential for homologous chromosome pairing during meiosis.[13] ZIP1 was the first TF protein identified in *S. cerevisiae*. It is a component of the central region of the SC and functions in initiation and chromosome synapsis, though its involvement in complete male sterility remains unclear.[15,33] In *Arabidopsis*, null mutants *zyp1−4*, *zyp1−5*, and *small organ 2* (*smo2*) revealed that *ZYP1* is crucial for crossover interference and is associated with significantly reduced fertility.[34] The allelic variation of *ZEP1* contributes to recombination, which plays a crucial role in the genetic diversity and evolution. Strong *zep1* alleles (e.g., *zep1−1* and *zep1−2*) are associated with low fertility and poor seed setting, while weak alleles (e.g., *zep1−3* and *zep1−4*) exhibit higher fertility and seed setting.[13] The strong alleles of *zep1* lead to partial sterility.[13] Similarly,

https://doi.org/10.1021/acs.jafc.5c09809
J. Agric. Food Chem. 2025, 73, 28143−28152

the week *zep1* allele, *zep1*−3, also causes partial sterility with approximately 35% seed setting.[14] Furthermore, *ZEP1* knockout in the CY84 hybrid, with a −1 bp insertion mutation (*zip1-KO*), caused sterility.[35] In this study, we reported that *MS4,* the strongest allele of *ZEP1,* causes complete male sterility in rice. We confirmed the *MS4* gene that was previously identified through a BLAST search using *Arabidopsis ZYP1,* and generated 89 fertile and 26 sterile self-fertilized heterozygous plants from the *zep1* mutant without mentioning fine mapping results.[13] Here, we fine-mapped *MS4* to the 49.8 kb region between markers KASP9 and KASP10 using 2054 individuals of $F_{2:3}$ populations (Figure 6), and validated that knock out of candidate gene *ZEP1* of *MS4* showed a complete male sterile phenotype using CRISPR/Cas9 (Figure 7).

The lipidic structures, cuticle, and pollen exine are indispensable for anther and pollen grain development and protection. The rice anther cuticle consists of two major components: the cutin matrix and waxes. After anther dehiscence, the exine forms the outer protective wall of the pollen.[3] Previously, *ZEP1* was not reported for pollen exine formation.[13,14,35] In this study, we isolated and characterized a complete male sterile mutant named *MS4*. The anther of the sterile line was relatively shorter, weaker, and pale yellow to whitish compared to the fertile (Figure 1C). The fertile pollen grains were larger and spherical, while the sterile pollen grains were shrunken and irregular (Figure 1E,F). Cytological observation revealed that the fertile anthers produced a normal cuticle and pollen exine compared with sterile anthers (Figure 3). The pollen exine of the fertile line was less compact and covered with sporopollenin, giving it a granular appearance, whereas the sterile pollen exine exhibited disorganized sporopollenin deposits (Figure 3). This suggests that defects in *ZEP1* affect pollen exine formation, but further investigations are needed.

The precise execution of cell division and cytokinesis is indispensable for growth and fertility. The genes *PRD1* and *PRD2* have been shown to affect spindle assembly in rice meiosis, resulting in unbalanced tetrads.[36,37] However, no genes of SC controlling male sterility have been found in connection with male sterility and tetrad formation until now. To determine whether complete male sterility results from defects in male meiosis, we investigated meiotic chromosomal behavior in male meiocytes from both fertile and sterile plants using DAPI staining (Figure 5). The sterile line exhibited not only abnormal cytokinesis in meiocytes but also irregular chromosome division. In the fertile line, dyads and tetrads at telophases I and II were normal, respectively, while in the sterile line, dyads at telophase I were normally condensed, but tetrads at telophase II were abnormal (Figure 5A,C). The fertile line exhibited equal-sized nuclei and cell mass at the dyad stage of male meiocytes, whereas the sterile line showed irregular triads with unequal nuclei of varying sizes and cell masses (Figure 5B,D). Additionally, *PAIR2* of SC led to partial triads during meiosis II due to the failure of homologous chromosome pairing.[8] These results suggest that defects in *MS4* disrupt cytokinesis and tetrad formation during male sporulation, leading to male sterility.

The *MS4* male sterility mechanism is relevant when a single recessive nuclear sterility gene controls the trait and the parental ILs unintentionally retain heterozygosity during backcrossing. The parental ILs may carry complementary fertility genes in different genomic regions (e.g., the S1/S2 system). When a specific gene combination (such as S1S2) occurs in the offspring, hybrid sterility may be triggered due to hybrid sterility gene interaction. This mechanism frequently occurs in reproductive isolation genes, such as hybrid sterility loci between Indica and japonica rice. Gene editing or molecular markers are needed for validation. Chromosomal structural variations and chromosome pairing abnormalities during meiosis in F_2 individuals may lead to aneuploid gametes, which result in sterility. Cytological analysis or whole-genome resequencing can be used to confirm structural variations.[2,38] Genetically engineered male sterility has diverse applications, ranging from hybrid seed production to the biocontainment of transgenes in genetically modified crops. This technology has already shown a significant impact across various crops, contributing to efforts to address global food security challenges. Furthermore, these conventional hybrid seed production methods are time-consuming and labor-intensive, limiting their broader application.[39] In our study, we identified a novel recessive gene with complete male sterility that holds promising potential for future applications in genetic engineering-based hybrid breeding systems.

■ ASSOCIATED CONTENT

Supporting Information

The Supporting Information is available free of charge at https://pubs.acs.org/doi/10.1021/acs.jafc.5c09809.

(Figure S1) SNP markers density per Mb in the 12 chromosomes of the rice genome genotyped using a 20 K chip assay; (Figure S2) comparison of sterility-related traits in fertile and sterile plants; (Figure S3) anther morphology of homozygous fertile and sterile plants; (Figure S4) genotypes of the IL (X-R), IL (U99), and heterozygous plants using KASP markers KASP9 and KASP10; (Table S1) genetic analysis of sterility trait in $F_{2:3}$ population using chi-square test. (Table S2) kompetitive allele-specific PCR (KASP) primers were used for fine mapping of *MS4*; (Table S3) primers used for genomic and promoter region sequencing of *ZEP1*; (Table S4) primer used for *ZEP1*-CRISPR/Cas9 (PDF)

■ AUTHOR INFORMATION

Corresponding Authors

Chengkai lu − *Key Laboratory of Tropical Plant Resources and Sustainable Use, Xishuangbanna Tropical Botanical Garden, Chinese Academy of Sciences, Mengla 666303, China; College of Life Sciences, University of Chinese Academy of Sciences, Beijing 101408, China*; Email: luchengkai@xtbg.ac.cn

Peng Xu − *Key Laboratory of Tropical Plant Resources and Sustainable Use, Xishuangbanna Tropical Botanical Garden, Chinese Academy of Sciences, Mengla 666303, China; College of Life Sciences, University of Chinese Academy of Sciences, Beijing 101408, China*; Email: xupeng@xtbg.ac.cn

Authors

Amir Sohail − *Key Laboratory of Tropical Plant Resources and Sustainable Use, Xishuangbanna Tropical Botanical Garden, Chinese Academy of Sciences, Mengla 666303, China*; orcid.org/0000-0002-3352-4957

Rongrong Qiao − *Key Laboratory of Tropical Plant Resources and Sustainable Use, Xishuangbanna Tropical Botanical Garden, Chinese Academy of Sciences, Mengla 666303,*

China; College of Life Sciences, University of Chinese Academy of Sciences, Beijing 101408, China

Xinyu Mao − *Key Laboratory of Tropical Plant Resources and Sustainable Use, Xishuangbanna Tropical Botanical Garden, Chinese Academy of Sciences, Mengla 666303, China*

Jinpeng Wan − *Key Laboratory of Tropical Plant Resources and Sustainable Use, Xishuangbanna Tropical Botanical Garden, Chinese Academy of Sciences, Mengla 666303, China; College of Life Sciences, University of Chinese Academy of Sciences, Beijing 101408, China*

Xiaochao Li − *Key Laboratory of Tropical Plant Resources and Sustainable Use, Xishuangbanna Tropical Botanical Garden, Chinese Academy of Sciences, Mengla 666303, China; School of Agriculture, Yunnan University, Kunming 650500, China*

Complete contact information is available at: https://pubs.acs.org/10.1021/acs.jafc.5c09809

Author Contributions

†A.S. and R.Q. contributed equally to this work.

Author Contributions

P.X. and C.L. designed the experiment. A.S. and R.Q. performed the experiment. A.S. wrote the paper. A.S., X.M., J.W., X.L., C.L., and P.X. revised the manuscript.

Funding

This work was supported by the grants from West Light Foundation of the Chinese Academy of Sciences (to P.X.), the Youth Innovation Promotion Association of the Chinese Academy of Sciences (2023412 to C.L.), Strategic Priority Research Program of the Chinese Academy of Sciences (grant no. XDA24040308), the 14th Five-Year Plan of the Xishuangbanna Tropical Botanical Garden, CAS (292023000131), Natural Science Foundation of Yunnan, China (grant no. 202301AT070351), the Major Science and Technology Project in Yunnan (202402AE090026), and the Yunnan Province Key Research and Development Plan Project (grant no. 202303AM140023).

Notes

The authors declare no competing financial interest.

REFERENCES

(1) Baxla, B.; Thiyagarajan, K.; Swaminathan, M.; Bellie, A.; Natarajan, S.; Govindan, S. K. Advances in two-line hybrid rice breeding: leveraging thermosensitive genetic male sterility system in rice for improved global rice production. *Euphytica* **2025**, *221*, 101.

(2) Abbas, A.; Yu, P.; Sun, L.; Yang, Z.; Chen, D.; Cheng, S.; Cao, L. Exploiting genic male sterility in Rice: from molecular dissection to breeding applications. *Front. Plant Sci.* **2021**, *12*, No. 629314.

(3) Zhang, D.; Luo, X.; Zhu, L. Cytological analysis and genetic control of rice anther development. *J. Genet. Genom.* **2011**, *38* (9), 379−390.

(4) Deng, Y.; Wan, Y.; Liu, W.; Zhang, L.; Zhou, K.; Feng, P.; He, G.; Wang, N. *OsFLA1* encodes a fasciclin-like arabinogalactan protein and affects pollen exine development in rice. *Theor. Appl. Genet.* **2022**, *135*, 1247−1262.

(5) Grienenberger, E.; Quilichini, T. The toughest material in the plant kingdom: an update on sporopollenin. *Front. Plant Sci.* **2021**, *12*, No. 703864.

(6) Ren, L.; Zhao, T.; Zhao, Y.; Du, G.; Yang, S.; Mu, N.; Tang, D.; Shen, Y.; Li, Y.; Cheng, Z. The E3 ubiquitin ligase DESYNAPSIS1 regulates synapsis and recombination in rice meiosis. *Cell Rep.* **2021**, *37* (5), No. 109941.

(7) Luo, Q.; Li, Y.; Shen, Y.; Cheng, Z. Ten years of gene discovery for meiotic event control in Rice. *J. Genet. Genom.* **2014**, *41* (3), 125−137.

(8) Nonomura, K. I.; Nakano, M.; Fukuda, T.; Eiguchi, M.; Miyao, A.; Hirochika, H.; Kurata, N. The novel gene *HOMOLOGOUS PAIRING ABERRATION IN RICE MEIOSIS1* of rice encodes a putative coiled-coil protein required for homologous chromosome pairing in meiosis. *Plant Cell* **2004**, *16* (4), 1008−1020.

(9) Nonomura, K.; Nakano, M.; Eiguchi, M.; Suzuki, T.; Kurata, N. PAIR2 is essential for homologous chromosome synapsis in rice meiosis I. *J. Cell Sci.* **2006**, *119* (2), 217−225.

(10) Yuan, W.; Li, X.; Chang, Y.; Wen, R.; Chen, G.; Zhang, Q.; Wu, C. Mutation of the rice gene PAIR3 results in lack of bivalent formation in meiosis. *Plant J.* **2009**, *59* (2), 303−315.

(11) Miao, C.; Tang, D.; Zhang, H.; Wang, M.; Li, Y.; Tang, S.; Yu, H.; Gu, M.; Cheng, Z. CENTRAL REGION COMPONENT1, a novel synaptonemal complex component, is essential for meiotic recombination initiation in Rice. *Plant Cell* **2013**, *25* (8), 2998−3009.

(12) Nonomura, K. I.; Nakano, M.; Murata, K.; Miyoshi, K.; Eiguchi, M.; Miyao, A.; Hirochika, H.; Kurata, N. An insertional mutation in the rice PAIR2 gene, the ortholog of *Arabidopsis ASY1*, results in a defect in homologous chromosome pairing during meiosis. *Mol. Genet. Genomics* **2004**, *271* (2), 121−129.

(13) Wang, M.; Wang, K.; Tang, D.; Wei, C.; Li, M.; Shen, Y.; Chi, Z.; Gu, M.; Cheng, Z. The central element protein ZEP1 of the synaptonemal complex regulates the number of crossovers during meiosis in Rice. *Plant Cell* **2010**, *22* (2), 417−430.

(14) Wang, K.; Wang, C.; Liu, Q.; Liu, W.; Fu, Y. Increasing the genetic recombination frequency by partial loss of function of the synaptonemal complex in rice. *Mol. Plant* **2015**, *8* (8), 1295−1298.

(15) Sym, M.; Engebrecht, J.; Roeder, G. ZIP1 is a synaptonemal complex protein required for meiotic chromosome synapsis. *Cell* **1993**, *72*, 365−378.

(16) de Vries, F. A. T.; de Boer, E.; van den Bosch, M.; Baarends, W. M.; Ooms, M.; Yuan, L.; Liu, J. G.; van Zeeland, A. A.; Heyting, C.; Pastink, A. Mouse *Sycp1* functions in synaptonemal complex assembly, meiotic recombination, and XY body formation. *Genes Dev.* **2005**, *19*, 1376−1389.

(17) Page, S.; Hawley, R. *c(3)G* encodes a Drosophila synaptonemal complex protein. *Genes Dev.* **2001**, *15*, 3130−3143.

(18) MacQueen, A.; Colaiacovo, M.; McDonald, K.; Villeneuve, A. Synapsis-dependent and -independent mechanisms stabilize homolog pairing during meiotic prophase in *C. elegans*. *Genes Dev.* **2002**, *16*, 2428−2442.

(19) Higgins, J. D.; Sanchez-Moran, E.; Armstrong, S. J.; Jones, G. H.; Franklin, F. C. H. The *Arabidopsis* synaptonemal complex protein ZYP1 is required for chromosome synapsis and normal fidelity of crossing over. *Genes Dev.* **2005**, *19* (20), 2488−2500.

(20) Barakate, A.; Higgins, J. D.; Vivera, S.; Stephens, J.; Perry, R. M.; Ramsay, L.; Colas, I.; Oakey, H.; Waugh, R.; Franklin, F. C. H.; Armstrong, S. J.; Halpin, C. The synaptonemal complex protein ZYP1 is required for imposition of meiotic crossovers in Barley. *Plant Cell* **2014**, *26* (2), 729−740.

(21) Golubovskaya, I.; Wang, C.; Timofejeva, L.; Cande, W. Maize meiotic mutants with improper or non-homologous synapsis due to problems in pairing or synaptonemal complex formation. *J. Exp. Bot.* **2011**, *62* (5), 1533−1544.

(22) Barakate, A.; Higgins, J. D.; Vivera, S.; Stephens, J.; Perry, R. M.; Ramsay, L.; Colas, I.; Oakey, H.; Waugh, R.; Franklin, F. C. H.; Armstrong, S. J.; Halpin, C. The synaptonemal complex protein ZYP1 is required for imposition of meiotic crossovers in barley. *Plant Cell* **2014**, *26*, 729−740.

(23) Khoo, K.; Able, A.; Able, J. The isolation and characterization of the wheat molecular ZIP per I homologue, TaZYP1. *BMC Res. Notes* **2012**, *5* (1), 106.

(24) Wang, F.; Lu, C.; Wan, J.; Yang, J.; Liu, L.; Zhang, F.; Wu, Z.; Zhang, X.; Chang, G.; Yu, D.; Xu, P. Genetic dissection of stem branch trait and envisioning of fixing heterosis by vegetative reproduction in *Oryza rufipogon*. *Agronomy* **2022**, *12*, 1503.

(25) Wu, Z.; Ji, J.; Tang, D.; Wang, H.; Shen, Y.; Shi, W.; Li, Y.; Tan, X.; Cheng, Z.; Luo, Q. *OsSDS* is essential for DSB formation in rice meiosis. *Front. Plant Sci.* **2015**, *6*, 21.
(26) Khan, R. M.; Yu, P.; Sun, L.; Abbas, A.; Shah, L.; Xiang, X.; Wang, D.; Sohail, A.; Zhang, Y.; Liu, Q.; Cheng, S.; Cao, L. *DCET1* controls male sterility through callose regulation, exine formation, and tapetal programmed cell death in rice. *Front. Genet.* **2021**, *12*, No. 790789.
(27) Luo, Z. Y.; Zhou, G.; Chen, X. H.; Lu, Q. H.; Hu, W. X. Isolation of high-quality genomic DNA from plants. *Bull. Hunan Med. Univ.* **2001**, *26*, 178−180.
(28) Miao, J.; Guo, D.; Zhang, J.; Huang, Q.; Qin, G.; Zhang, X.; Wan, J.; Gu, H.; Qu, L. J. Targeted mutagenesis in rice using CRISPR-Cas system. *Cell Res.* **2013**, *23*, 1233−1236.
(29) Hiei, Y.; Komari, T.; Kubo, T. Transformation of rice mediated by Agrobacterium tumefaciens. *Plant Mol. Biol.* **1997**, *35*, 205−218.
(30) Broman, K.; Wu, H.; Sen, S.; Churchill, G. A. R/qtl: QTL mapping in experimental crosses. *J. Bioinform.* **2003**, *19* (7), 889−890.
(31) Sohail, A.; Lu, C.; Xu, P. Genetic and molecular mechanisms underlying the male sterility in rice. *J. Appl. Genetics* **2025**, *66* (2), 251−265.
(32) Xu, Y.; Yu, D.; Chen, J.; Duan, M. A review of rice male sterility types and their sterility mechanisms. *Heliyon* **2023**, *9* (7), No. e18204.
(33) Storlazzi, A.; Xu, L.; Schwacha, A.; Kleckner, N. Synaptonemal complex (SC) component Zip1 plays a role in meiotic recombination independent of SC polymerization along the chromosomes. *Proc. Natl. Acad. Sci. U.S.A.* **1996**, *93*, 9043−9048.
(34) Capilla-Perez, L.; Durand, S.; Hurel, A.; Lian, Q.; Chambon, A.; Taochy, C.; Solier, V.; Grelon, M.; Mercier, R. The synaptonemal complex imposes crossover interference and heterochiasmy in *Arabidopsis*. *Natl. Acad. Sci. USA* **2021**, *118*, No. e2023613118.
(35) Liu, C.; Cao, Y.; Hua, Y.; Du, G.; Liu, Q.; Wei, X.; Sun, T.; Lin, J.; Wu, M.; Cheng, Z.; Wang, K. Concurrent disruption of genetic interference and increase of genetic recombination frequency in hybrid Rice using CRISPR/Cas9. *Front. Plant Sci.* **2021**, *12*, No. 757152.
(36) Shi, W.; Ji, J.; Xue, Z.; Zhang, F.; Miao, Y.; Yang, H.; Tang, D.; Du, G.; Li, Y.; Shen, Y.; Cheng, Z. PRD1, a homologous recombination initiation factor, is involved in spindle assembly in rice meiosis. *New Phytol.* **2021**, *230* (2), 585−600.
(37) Wang, C.; Qu, S.; Zhang, J.; Fu, M.; Chen, X.; Liang, W. *OsPRD2* is essential for double-strand break formation, but not spindle assembly during rice meiosis. *Front. Plant Sci.* **2023**, *13*, 1122202.
(38) Moon, S.; Lee, Y.; Gutierrez-Marcos, J.; Jung, K. H. Advancements in hybrid rice production: improvements in male sterility and synthetic apomixes for sustainable agriculture. *Plant Biotechnol. J.* **2025**, *23*, 2330−2345.
(39) Du, M.; Zhou, K.; Liu, Y.; Deng, L.; Zhang, X.; Lin, L.; Zhou, M.; Zhao, W.; Wen, C.; Xing, J.; Li, C. B.; Li, C. A biotechnology-based male-sterility system for hybrid seed production in tomato. *Plant J.* **2020**, *102* (5), 1090−1100.

https://doi.org/10.1021/acs.jafc.5c09809
J. Agric. Food Chem. 2025, 73, 28143−28152